Available online at www.sciencedirect.com
ScienceDirect
International Journal of Thermal Sciences 47 (2008) 293–305
International Journal of Thermal Sciences
www.elsevier.com/locate/ijts

Study of the behaviour of a flame resulting from the combustion of pine needles in a cylindrical basket

M. Saâdaoui [a], N. Mahjoub Saïd [b], H. Mhiri [a], Ph. Caminat [c], G. Le Palec [c,*], Ph. Bournot [c]

[a] *Ecole Nationale d'Ingénieurs de Monastir, Tunisia*
[b] *Faculté des sciences de Monastir, Tunisia*
[c] *CIME, Equipe IMFT, UNIMECA, Marseille, France*

Received 3 July 2006; received in revised form 11 January 2007

Available online 23 February 2007

Abstract

This experimental and numerical study examines the behaviour of a flame resulting from the combustion of pine needles. The objective of this work is to evaluate the performances of two models of combustion, the validity of these being discussed by comparing the results with experimental measurements. An apparatus was designed to simulate and study in laboratory conditions the flame and the near-field plume stemming from the combustion of an isolated shrub. The burner was made of a cylindrical wire mesh basket filled with pine needles ignited at the lower circumference of the basket. Particle Image Velocimetry (PIV) and Laser Doppler Anemometry (LDA) were used to characterize the velocity field in the proximity of the fuel and to identify the propagation of the flame. A set of time-dependent equations is obtained for each phase and the coupling between the gas phases is rendered through exchange terms of mass, momentum and energy. Turbulence is approached by using a k–ε statistical model constructed from the Favre averaging method. The chemical kinetics is assumed as infinitely fast compared with other characteristics of the flow. Two models of turbulent combustion are tested. The first is the EDC model, which considers an immediate reaction and the direct transformation of fuel into water and carbon dioxide. The second is the β-PDF model, which is based on an instantaneous thermodynamic equilibrium at any point. The solution is performed numerically by a finite-volume method. The numerical results obtained are presented and compared to experimental measurements.

Keywords: Experimental/numerical study; Flame; Combustion; Pine needles; EDC model; β-PDF model

1. Introduction

Vegetation is a polyphase and multi-constituent complex medium in which the development and the propagation of a fire are subject to physical mechanisms. These mechanisms may be studied on a mesoscopic, macroscopic or microscopic scale [1, 2]. The study of energy transfer associated with the propagation of the fire is particularly relevant to fire-protection strategy, and it enables the determination of weather conditions in which a habitation is likely to ignite, as well as the distance the fire is likely to spread.

Simulation of forest fire propagation can serve several purposes. The prediction of the fire front can help firefighters to optimise the distribution of fighting means, which requires real time simulation. Another application of simulation relates to fire prevention. Using terrain data, computer models of propagation could provide information on dangerous areas. The possibility for such models to take into account some aspects of the means of fire fighting, such as chemical retardants, should be highly desirable.

Currently, however, fire spreading simulators are far from being scientifically satisfactory. The reason is that forest fire is a complex large-scale natural phenomenon that is influenced by both the chemico-physical aspects of the combustion of the forest stratum that produces heat, and the local meteorological forecast.

* Corresponding author.
E-mail addresses: Mahjoub_nejla@yahoo.fr (N. Mahjoub Saïd), Georges.lepalec@univmed.fr (G. Le Palec).

1290-0729/$ – see front matter
doi:10.1016/j.ijthermalsci.2007.01.021

Nomenclature

Cp_s^k	specific heat of solid particles family (k)
C_{ref}	coefficient of the Sutherland's law
$F_{s,i}$	drag force resulting from gas/particles interaction in the fuel bed
g_i	gravity acceleration in the i-direction
h	enthalpy of the gas mixture
h_{conv}	gas/particle heat transfer coefficient
I	radiative intensity
J	total irradiance
k	turbulent kinetic energy
$\dot{M}_{s,\alpha}$	production term of species α resulting from the decomposition of the solid particles
P_g	pressure of the gas mixture
P_k	turbulent shear
Pr	Prandtl number
Q_{conv}^k	gas/particles convective heat transfer
Q_{rad}^k	gas/particles and particles/particles radiative heat transfer
R_0	universal gas constant
t	time
T	temperature of the gas mixture
T_s^k	temperature of the solid particles
x	height of the flame
x_i	Cartesian coordinate in the i-direction
u_i	velocity vector component in the i-direction
W_k	buoyancy turbulent production terms
W_α	molecular weight
y	radial distance along the y axis
$Y_{s,i}^k$	mass fraction of dry wood
$Y_{s,\text{H}_2\text{O}}^k, Y_{s,\text{char}}^k$	moisture content, and char of solid particles
Y_α	mass fraction of species α

Greek symbols

α_g, α_s	volume fraction of the gas and solid phase
Δh_{char}	reaction heat charcoal oxidation
ε	rate of dissipation of turbulent kinetic energy
μ_g	viscosity of the gas mixture
μ_t	eddy viscosity
μ_α	viscosity of each chemical species
ρ_g, ρ_s^k	density of the gas and solid phases
σ	Stefan–Boltzmann constant
σ_g	absorption coefficient of the gas/soot mixture
σ_{ij}	stress tensor
σ_s^k	surface area/volume ration of solid particles
$\dot{\omega}_\alpha$	rate of production, destruction rate of species α (combustion)
$\dot{\omega}_{s,\text{pyr}}^k, \dot{\omega}_{s,\text{vap}}^k$	pyrolysis and drying reaction rates
$\dot{\omega}_{s,\text{char}}^k$	rate of oxidation of charcoal
φ	heat flux density received by the vertical planes

These two aspects are coupled together because wind activates fire and fire is a heat source that induces convection above the forest. The topography of the landscape is very important for forest fire prediction as well. Much of the difficulty of modelling forest fires concerns the description of the physical mechanisms taking place inside the vegetal stratum.

Fire propagation in heterogeneous combustible media is the result of transfers between a gaseous phase (air and/or combustion products) and solid particles.

Rothermel's model [3] gives the fire heat source and the fire straight front velocity as analytical empirical laws for a uniform forest.

There have been a number of studies attempting to model fire spread through a fuel bed. A classification and discussion of the mathematical models developed up until 1991 can be found in the paper of Weber [4] completing the survey of Catchpole and De Mestre [5]. These models were classified as statistical, empirical and physical models according to whether they involve no physics at all, no distinction between different modes of heat transfer (conduction, convection, and radiation) or account for each mechanism of heat transfer individually. In the statistical models, the fire spread rate is predicted without involving any physical mechanisms, whereas the empirical models are based on the physical principle of conservation of energy, but do not differentiate between modes of heat transfer. In the physical models, the modes of heat transfer are differentiated and the fire spread rate along a given direction is found by solving a one-dimensional steady energy equation (see, for example, Refs. [6, 7]) or a bidimensional one [8]. They differ mainly owing to the heat transfer mechanisms involved in their formulation: ember radiation, flame radiation, convective transfer between the gas and solid phases, heat losses. The necessary input data are the topology of the combustible medium (density, surface area per unit volume, etc.), the thermochemical properties of the fuel material, and the ignition criteria. In addition, reduced models are developed in order to describe such phenomena as ember or flame radiation, heat losses, and convective transfer between gas and solid particles. Therefore, parameters such as the geometry of the flame (size, angle of inclination), convection heat transfer coefficient between gas and particles have to be known. These parameters are often difficult to obtain, and may vary from one situation to another.

Flame shape can also be modified by the aerodynamic structure of the environment in which the fire develops, but these models are not capable of modelling such fire-aerodynamic interactions.

Complete forest fire physical models taking better account of physical mechanisms taking place inside the vegetal stratum have been proposed by Grishin [9] and Larini et al. [10]. These models are based upon global equilibrium laws of mass energy and momentum. They consider the forest as a porous medium, composed of a gaseous phase and a vegetal phase, i.e. the wood, the stacks, the leaves, etc., in which transfer of mass, energy and momentum takes place. With these two physical models

great effort has been exerted in modelling combustion in the vegetation.

The set of equations given in Grishin's model is postulated on both basic half-scale experimental data and physical equilibrium laws governing transfer in porous media. This model is closed and is adequate for the prediction of general forest fire propagation. The closure is obtained by physical intuition and experimental observations.

Nevertheless, it is very difficult to derive physical laws from laboratory experiments such that the similarity conditions are satisfied. On the other hand, the model of Larini et al. is derived using the formal averaging method and the closure is obtained after some restrictive assumptions, for example that the gaseous heat conduction is negligible, and invoking some empirical laws. Moreover, the derived set of equations is not closed because coupled small-scale flow resolution is still needed.

It is therefore of interest to undertake a new derivation of a closed set of equations for the combustion inside the forest, similar to that of Grishin, by use of a general closing tool, i.e. by the derivation of a combustion model of forest vegetation.

Linn et al. [11] described turbulence on three different scales corresponding to three relevant fuel structure sizes, and used a probability distribution function (PDF) for the calculation of the solid-phase temperature. The treatment of combustion and radiation processes was simplified.

Morvan et al. [12] describe in their work the physical behaviour and the propagation of a small-scale surface fire in pine needle litter. The model developed is based on a multiphase approach and includes the main basic physical mechanisms. The studied cases are limited to a two-dimensional configuration. This assumption can be justified considering that the observations show that the widths of many spreading fires are in nature much greater than the fire depth. Although the flames exhibit fully three-dimensional behaviour, the major contributions concerning the heat equilibrium inside the fuel bed and above the litter can be treated as two-dimensional over shorter portions of the fire front.

The moisture in the vegetation represents a limiting factor for the spread of a fire. In a bed of pine needles, a moisture content greater than 13% was found to be enough to stop the fire from propagating [9,13]. It is important to note that the semi-empirical Rothermel model [3] proposed a threshold moisture content of 30%. The question remains how a wildfire can sustain propagation through a combustible layer of living vegetation characterized by moisture content above 70%. In this case the spread of a fire is sustained by the presence of dead fuel (moisture content $<10\%$), which burns very easily and lights the remainder of the combustible layer. Experimental fires through a mixture of two solid fuels (sticks + excelsior) [14] showed that, in spite of the very significant role played by the thinnest fuel (excelsior), the rate of spread of a fire in a mixture of fuels was much lower than that observed in the excelsior only. For all these reasons, the description of the fuel must take into account the thinnest particles, as well as the dead fuel, even if the latter represents a small fraction of the biomass.

The propagation of wildfire through a Mediterranean shrub has been numerically simulated using a multiphase formulation by Morvan et al. [15]. The heterogeneous character of the vegetation (nature, foliage, twigs, trunk, etc.) was taken into account using families of solid particles, which are characterized by specific physical properties. The interaction between dead and living fuel, which plays a significant role in the propagation of a wildfire, was taken into account. The calculations were performed for a surface fire propagating through Mediterranean vegetation. The results show the effects of wind on heat transfer between the fire front and the vegetation. Two modes of fire propagation are identified: plume-dominated fires and wind-driven fires, respectively dominated by radiation and convection heat transfer.

We performed, in this work, an experimental procedure in order to study the propagation of a flame resulting from the combustion of pine needles placed in a cylindrical basket, and we also used a numerical multiphase approach (solid phases representing the mixture of the vegetation + gas). The numerical study developed in this present paper is based on the resolution of the conservation equations (mass, species, momentum, energy) that govern the behaviour of the coupled system formed by the solid fuel particles and the gas mixture during the propagation of the fire.

By comparing experimental results with numerical ones, the performances of two models of turbulent combustion are tested: the Eddy Dissipation Concept (EDC) model, which is an extension of the Eddy Break-Up model [16,17] in which the phenomenon of combustion is described with only one irreversible chemical reaction, being controlled by the turbulent mixture. The second is the β-PDF model [18,19]: the flow is considered to have instantaneous chemical equilibrium at any point. This is carried out by means of the transport of a passive scalar—i.e. the mixture fraction—controlled by the turbulent mixture. This fraction represents the chemical equilibrium state at any point of the flow.

2. Experimental study

In our study, we were interested in the behaviour of a flame resulting from the combustion of pine needles which were placed in a basket, the dimensions of which were 10 cm diameter and 10 cm height. The experiments were performed in a 6 m × 5 m × 9 m room with one opening for the smoke exit. Fuel was made of oven-dried pine needles. It was ignited at the lower circumference of the basket using alcohol. We used identical dried pine needles for all our tests. Their main characteristics were: length 10 cm, average thickness 1.18 mm. The initial moisture content was about 10%. The pine needles were dried at a temperature of 60 °C for 24 h in a drying oven. For each test, the mass of pine needles was 10 g. The balance had a precision of 0.1 g. Each solid phase consisted of particles with the same geometrical (e.g., shape and size) and thermochemical properties, thus providing the same behaviour under fire. The pine needles were spread as uniformly as possible.

The experimental device is shown in Fig. 1. During the experiments, the evolution of the mass of needles was measured by means of a balance connected to a data acquisition station. The temperature was measured by means of two

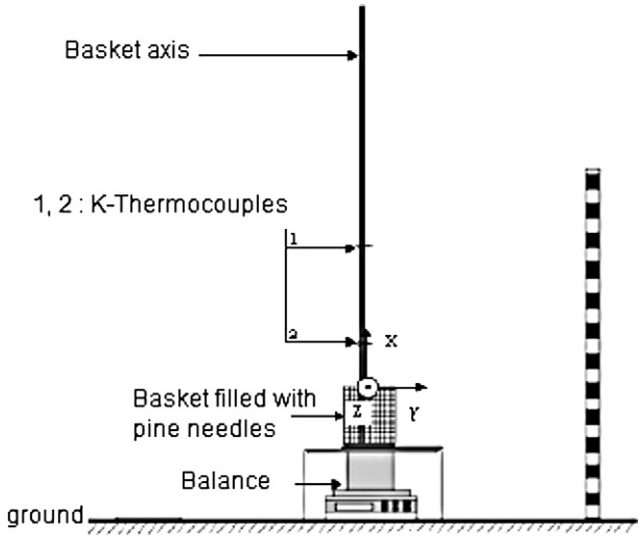

Fig. 1. Experimental device.

K-thermocouples with diameter 0.175 mm and usable in the range −270 to 1370 °C. The thermocouples had a precision of 1 °C. Estimates of the error of temperature measurement due to the radiation lost by the thermocouples were always below 10% [20].

The thermocouples were also connected to the same data acquisition station so that the temperature and mass evolution were managed by the same computer.

The thermocouples were located at different heights x from the top of the basket.

The two thermocouples TC were moved along the vertical axis during the experiment to record temperatures at different heights.

2.1. Seeding

It must be emphasized that the techniques used for these measurements are non-invasive. However, they require the presence, within the fluid, of particles whose displacements will be measured.

Our work is based on the hypothesis that particles follow the flow, and that their velocities are identical to that of the fluid. Combustion provides part of the seeding, which is supplemented by two other seeders: the first one is a smoke generator, whose particles are meant to seed the ambient air in the test section. The second one generates mono-dispersed vegetal oil droplets, which are sprayed under the pine needles at the lower circumference of the basket to add more particles to the flame.

2.2. Velocity measurements

To quantify the velocity field, two techniques were applied (Fig. 2).

2.2.1. Particle Image Velocimetry (PIV)

The purpose of PIV is to establish charts of velocity vectors in a region of the flow. This region is lit with a laser and filmed with a CCD camera assembled on a telescopic support. The system consists of a high-resolution camera (1600 × 1200 pixels) connected to a computer. The light sheet is generated by a dual YAG laser with a 10 Hertz pulse rate (10 velocity fields per second) and a pulse separation between 100 ns and 10 ms.

For velocities of the order of 1 to 10 $\mathrm{m\,s^{-1}}$, the signal-sampling rate will be in the range of 2–20 MHz.

2.2.2. Laser Doppler Anemometry (LDA)

This method makes it possible to measure two instantaneous velocity components at a point of the flow. The lasers used

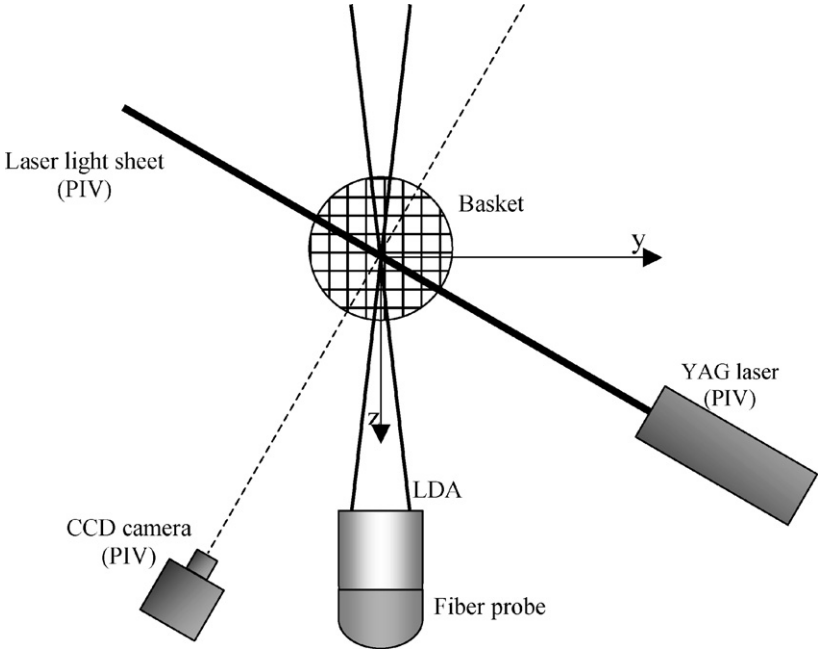

Fig. 2. Experimental LDA and PIV set-up (top view).

are connected to a data-processing power station which records data and allows the analysis of measurements. The laser was fixed on a mobile rail which allows vertical and horizontal displacements.

The uncertainties were about 5%. The estimates were inferred from estimated inaccuracies in the calibration data and from the observed scatter in the measurements.

The tests were carried out at ambient temperature and atmospheric pressure. The reproducibility of the results is not assured, so that the experiment was carried out five times in the same climatic conditions (temperature, pressure and moisture) and for the same mass of pine needles. The experimental results presented in this paper are the averages of the results obtained for the five tests.

3. Theoretical approach

We propose to study the propagation of a flame through pine needle fuel in a cylindrical basket. The fuel is represented as an initially homogeneous distribution of cylindrical particles whose dimensions are evaluated from experimental data. Consideration is given to an unsteady, three-dimensional and turbulent flow. The Cartesian coordinate system used here is centred at the basket's upper surface.

The physical properties are identical to those retained for the experiments carried out in the laboratory [21]. The numerical parameters used in the calculation are: specific heat 1337 $\mathrm{J\,kg^{-1}\,K^{-1}}$, density 680 $\mathrm{kg\,m^{-3}}$ [22].

In order to give a mathematical description of the experiments, the following assumptions were made:

- the gas reactive medium satisfies the law of perfect gases,
- the mass diffusion coefficients are the same for all the species, as well as the specific heats,
- the Soret and Dufour effects as well as the barometric diffusion are negligible,
- the Mach number is low,
- the Lewis number is equal to the unit ($Le = 1$).

3.1. Equations for the gaseous phase

The behaviour of the gas mixture resulting from the thermal degradation of the vegetation and the combustion reactions is governed by the generalized Navier–Stokes equations. According to the magnitudes of the velocity and length scales of this problem, the flow was expected to be turbulent in some region of the computational domain (above the fire front, in the plume zone, etc.). To render the average behaviour of the gaseous phase, the equations describing the evolution of the turbulent flow were filtered in time using a mass-weighted average (Favre) formulation [23,24]. The double correlation terms representing the effects upon the average flow induced by the fluctuations were approximated using Boussinesq's eddy viscosity concept and the generalized approximation of gradient diffusion. After this mathematical treatment, the average mass, momentum, and energy balance equations in the gas phase can be written as:

$$\frac{\partial(\bar{\rho})}{\partial t} + \frac{\partial(\bar{\rho}\tilde{u}_j)}{\partial x_j} = \overline{\sum_{\alpha,k} \dot{M}^k_{s,\alpha}} \tag{1}$$

$$\frac{\partial(\bar{\rho}\tilde{u}_i)}{\partial t} + \frac{\partial(\bar{\rho}\tilde{u}_j\tilde{u}_i)}{\partial x_j} = \frac{\overline{\partial(\alpha_g\sigma_{ij})}}{\partial x_j} - \frac{\overline{\partial(\rho u''_j\rho''_i)}}{\partial x_j} + \bar{\rho}g_i - \overline{\sum_k F^k_{s,i}} \tag{2}$$

$$\text{with } \bar{\sigma}_{ij} = -\bar{\rho}\delta_{ij} + \bar{\mu}\left[\frac{\partial\tilde{u}_i}{\partial x_j} + \frac{\partial\tilde{u}_j}{\partial x_i} - \frac{2}{3}\frac{\partial\tilde{u}_k}{\partial x_k}\delta_{ij}\right]$$

$$\begin{aligned}\frac{\partial(\bar{\rho}\tilde{h})}{\partial t} &+ \frac{\partial(\bar{\rho}\tilde{u}_j\tilde{h})}{\partial x_j} \\ &= \overline{\frac{\partial}{\partial x_j}\left(\frac{\mu}{Pr}\frac{\partial T}{\partial x_j}\right)} - \frac{\overline{\partial(\rho u''_j h'')}}{\partial x_j} - \overline{\sum_k Q^k_{\mathrm{conv}}} + \frac{\overline{\partial(\alpha_g P)}}{\partial t} \\ &\quad + \overline{\alpha_g\sigma_g\left(J - 4\sigma T^4\right)} + \overline{\sum_{\alpha,k}\dot{M}^k_{s,\alpha}h_{s,\alpha}} \\ &\quad + (1-\alpha_{sg})\Delta h_{\mathrm{char}}\overline{\sum_k \dot{\omega}^k_{s,\mathrm{char}}}\end{aligned} \tag{3}$$

$$\frac{\partial(\bar{\rho}\tilde{Y}_\alpha)}{\partial t} + \frac{\partial(\bar{\rho}\tilde{u}_j\tilde{Y}_\alpha)}{\partial x_j} = \overline{\frac{\partial}{\partial x_j}\left(\frac{\mu}{Pr}\frac{\partial Y_\alpha}{\partial x_j}\right)} - \frac{\overline{\partial(\rho u''_j Y''_\alpha)}}{\partial x_j} + \bar{\dot{\omega}}_\alpha + \overline{\sum_k \dot{M}^k_{s,\alpha}} \tag{4}$$

where: $\rho = \alpha_g\rho_g$; $\mu = \alpha_g\mu_g$; $P = \alpha_g P_g$.

The subscript g refers to gas properties, the superscripts (–), (∼), and ($''$) denote time average, density-weighted Favre average and density-weighted Favre fluctuation.

All the main parameters are defined in the nomenclature. $F^k_{s,i}$ is the ith component of the drag force and Q^k_{conv} is the convective heat flux between the gas and particles. These parameters and the equation of state with the assumption of perfect gases are reported in [12].

The introduction of the fluctuating entities makes this system open. Its closing requires the use of a model of turbulence which makes it possible to obtain a number of equations equal to the number of unknown factors. For this study, we used the first order standard k–ε closure model [25].

3.2. Equations for the solid phase

Under the action of heat released by the fire, the temperature of solid fuel particles (T^k_s) increases. This temperature rise first causes the evaporation of water, and then the volatilization of the dry material, producing a flammable mixture of gaseous products (pyrolysis) and the conversion of the remaining solid fuel to charcoal. During this degradation process the state of the fuel particles was described using the mass fraction of water ($Y^k_{s,\mathrm{H_2O}}$), dry material ($Y^k_{s,i}$), charcoal ($Y^k_{s,\mathrm{char}}$), and ash. The time evolution of these variables was calculated solving the conservation equations for mass, species, and energy written for each solid phase (k) as follows [12,15]:

$$\frac{d}{dt}\left(\alpha_s^k \rho_s^k Y_{s,\mathrm{H_2O}}^k\right) = -\dot{\omega}_{s,\mathrm{vap}}^k \tag{5}$$

$$\frac{d}{dt}\left(\alpha_s^k \rho_s^k Y_{s,i}^k\right) = -\dot{\omega}_{s,\mathrm{pyr}}^k \tag{6}$$

$$\frac{d}{dt}\left(\alpha_s^k \rho_s^k Y_{s,\mathrm{char}}^k\right) = (\nu_{\mathrm{char}} - \nu_{\mathrm{soot}})\dot{\omega}_{s,\mathrm{pyr}}^k - \left(\frac{\nu_{\mathrm{ash}}}{\nu_{\mathrm{char}}} + 1\right)\dot{\omega}_{s,\mathrm{char}}^k \tag{7}$$

These expressions allow writing the conservation of mass for the solid particles as:

$$\frac{d}{dt}\left(\alpha_s^k \rho_s^k\right) = -\sum_{\alpha} \dot{M}_{s,\alpha}^k = (\nu_{\mathrm{char}} - \nu_{\mathrm{soot}} - 1)\dot{\omega}_{s,\mathrm{pyr}}^k - \dot{\omega}_{s,\mathrm{vap}}^k - \dot{\omega}_{s,\mathrm{char}}^k \tag{8}$$

$$\frac{d}{dt}\left(\alpha_s^k\right) = -\frac{1}{\rho_s^k}\dot{\omega}_{s,\mathrm{char}}^k \tag{9}$$

and the conservation equation of energy for the solid phase:

$$\alpha_s^k \rho_s^k C p_s^k \frac{dT_s^k}{dt} = \bar{Q}_{\mathrm{conv}}^k + \bar{Q}_{\mathrm{rad}}^k - \sum_{\alpha} \dot{M}_{s,\alpha}^k h_{s,\alpha} + \alpha_{s,g}\Delta h_{\mathrm{char}}\dot{\omega}_{s,\mathrm{char}}^k \tag{10}$$

$$\bar{Q}_{\mathrm{conv}}^k = h_{\mathrm{conv}}\alpha_s^k \sigma_s^k\left(T - T_s^k\right) \tag{11}$$

$$\bar{Q}_{\mathrm{rad}}^k = \frac{\alpha_s^k \sigma_s^k}{4}\left(J - 4\sigma {T_s^k}^4\right) \tag{12}$$

The particles are assumed to be motionless during the major part of pyrolysis and combustion, except at the end of the decomposition where the formation of ashes occurs. When the particles are completely transformed into ashes, the interactions between gas and particles can be neglected.

Radiation is one of the most important heat transfer mechanisms during the propagation of a fire. Radiation mainly results from soot particles produced in the flame and from the embers situated behind the fire front [26].

3.3. The combustion model description

In our paper we used two models of combustion. The first model (the EDC model [16,17]) considers an immediate reaction and the direct transformation of fuel into water and carbon dioxide. The EDC combustion model considers that the chemical kinetics is infinitely fast compared with other characteristics of the flow [16], and that the rates of appearance or disappearance of chemical species are controlled by turbulence. The second model (β-PDF model) uses a thermodynamic equilibrium in any point and at every moment [18,19]. In contrast to the preceding model, this model considers that the flow is in chemical equilibrium at any point and at any time. This is carried out by means of a passive scalar, f (fraction of mixture) which is controlled by the turbulent mixture.

All the transport equations are discretized on a non-uniform grid using the finite volume method. The method consists of integrating equations on each control volume. The resulting systems of linear algebraic equations for each variable are then solved iteratively using a TDMA algorithm [27]. To procure convergence, all the variables are under-relaxed using inertial relaxation.

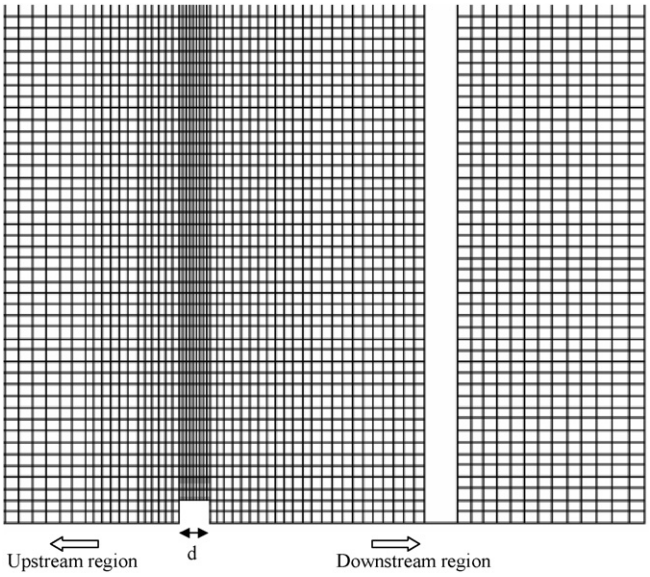

Fig. 3. Schematic presentation of the grid at the symmetry plane.

Different grid sizes were tested to ensure that the solution was independent of grid density.

The variation of the mesh size is described by the following relation: $x_{i+1} = x_i + \alpha_x \Delta$. Indeed, the step of calculation and the rate of extension of the grid in the longitudinal direction are taken equal to $\Delta = 0.8$ cm and $\alpha_x = 0.98$, upstream of the basket, respectively.

Near the basket, these are reduced to $\Delta = 0.3$ cm and $\alpha_x = 1$ (Fig. 3). Downstream of the basket, values of $\Delta = 1.3$ cm and $\alpha_x = 0.98$ are adopted. This grid is refined around the basket. In the transverse and lateral directions, the mesh size is uniform with a constant step equal to 0.8 cm. For all directions, the number of points is chosen so that the boundary conditions far from the flame are satisfied.

Several steps of time were tested for different step of space and the results obtained are not modified starting from a step of time $= 10^{-2}$ s.

The iterative process stops when the convergence criterion defined as: $|\frac{\phi^{m+1} - \phi^m}{\phi^{m+1}}| \leqslant 10^{-5}$ is satisfied, where ϕ represents a transported quantity and m is the iteration number.

4. Results and discussion

After ignition of the pine needles at the lower circumference of the basket, small flames develop vertically up to about the top of the basket. The pine needles are first heated because, upstream from the flame, the needles receive energy mainly by radiation and convection. The temperature increases until it reaches the boiling point of water. Once the water contained in the fuel is completely evaporated, the temperature again increases. Therefore, the combustion spreads through the fuel along the vertical sides of the basket very fast. Then the combustion mainly spreads from the circumference to the centre of the basket, while one single flame devel-

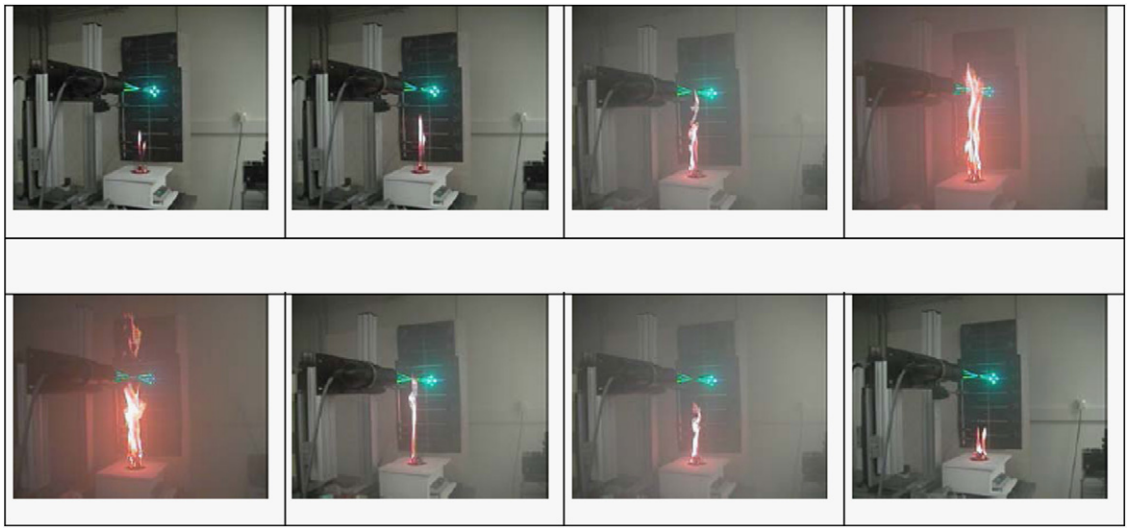

Fig. 4. Instantaneous visualization of the flame propagation.

ops above.The characteristic red colour of embers (i.e., char combustion) appears after complete extinction of the yellow flames above the fuel. The fuel is finally reduced completely to ashes.

4.1. Height of the flame

In Fig. 4, we present photographs showing the evolution of the flame from lighting to extinction. After the firing of the fuel, the flame grows gradually in height until it reaches a limiting value ranging between 60 and 80 cm. The increase of the flame height causes an acceleration of the pyrolysis rate and an increase in the quantity of fresh air consumed by the burning zone. These two phenomena induce, respectively, a heating and a cooling of the solid particles located ahead of the fire. It is the combination of these two contradictory effects which is at the origin of the oscillatory behaviour observed in experiments. Then, the flame decreases appreciably until there remains only the combustion of embers. The extinction of the fire then occurs for lack of fuel.

4.2. LDA measurements

The axial and transverse velocity profiles measured through the LDA technique are presented in Fig. 5 at $x = 30$ cm on the vertical axis as a function of time t.

During the first stage, the average value of the velocity is about 0.6 m s^{-1}. Then the fire propagates through the entire fuel basket. A steady state is reached and the final average propagation velocity is about 2.5 m s^{-1}. We note that the fire propagates but slows down after a few minutes and finally stops when the ignition ends.

4.3. PIV measurements

A pine needle flame is generally a dynamic phenomenon that changes its behaviour with the passage of time. The flame will propagate and grow both in size and intensity.

Fig. 6 reveals the unsteady stages of flame propagation. They present the different phases of development and propagation regimes of the flame.

This figure shows an example of the time evolution of the instantaneous flame height. A maximum height was reached a few seconds after the maximum rate of mass loss. This example shows that despite a non-steady combustion regime, a stage of quasi-steady and fully developed flame was observed. We also note the oscillatory behaviour of the flame. The duration of this stage depends on the combustion regime. Then, the flame decreases appreciably until there remains only the combustion of embers. At the end of the process, the extinction of the fire occurs for lack of pine needles in the cylindrical basket.

4.4. Loss of mass of the pine needles

The progressive loss of mass during the combustion of the pine needles is represented in Fig. 7. This degradation occurs in an almost linear way during the first 50 seconds. The curve then shows a flat section which indicates that all the needles were burned. Moreover, it is interesting to note that this 50 seconds duration coincides well with the beginning of the progressive fall in temperature recorded by the thermocouples from this same moment.

In Fig. 7 we compare the experimental data with the numerical results obtained from the two models of combustion. We notice that the loss of mass obtained from the EDC model is much faster than that obtained from the experimental data. This is explained by the fact that the EDC model considers an immediate reaction and thus a faster combustion. On the other hand, a quasi-perfect agreement is observed between the results given by the β-PDF model and those obtained from the experimental data.

For a more detailed study of the loss of mass, and in order to distinguish the three phases described previously (Fig. 4), it seems that the derivative of the loss of mass according to time translates as the various stages of the evolution of the flame (Fig. 8).

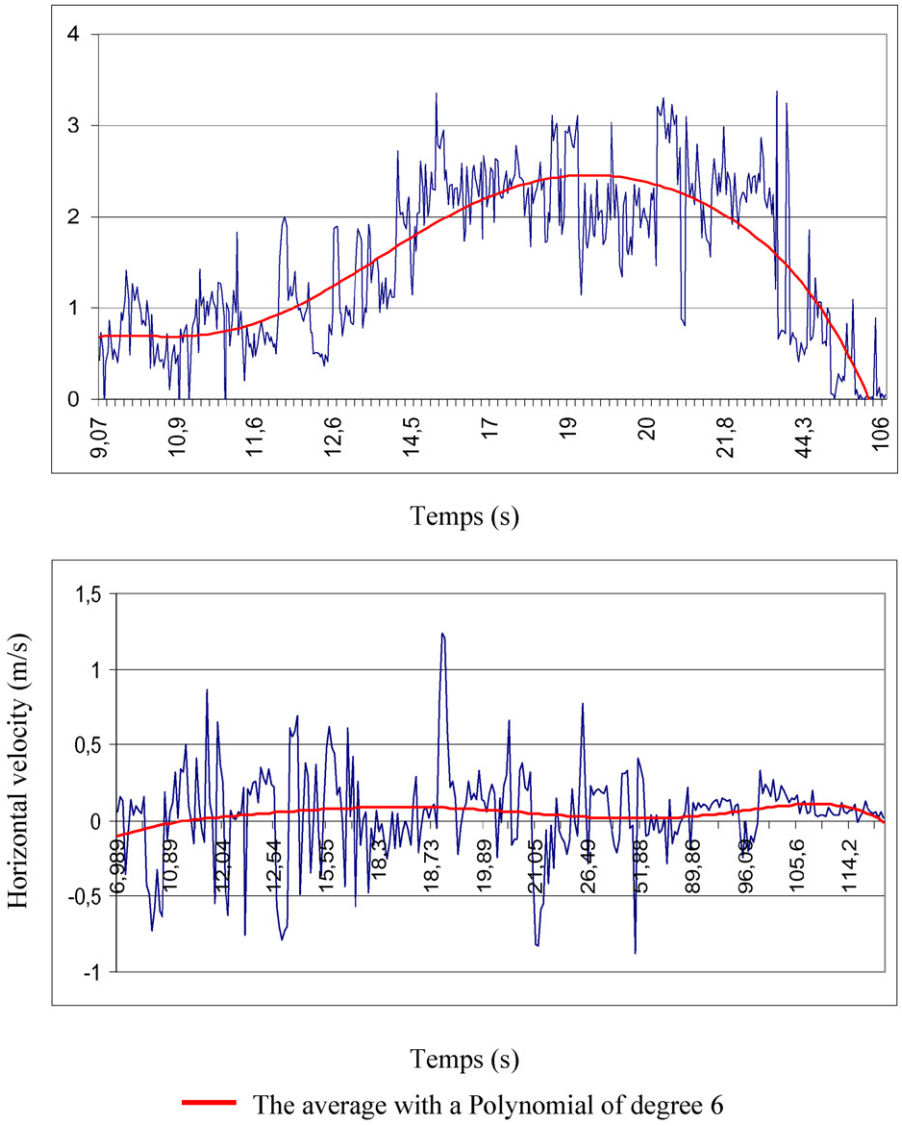

Fig. 5. The velocities measured through LDA at a height $x = 30$ cm.

We note that from $t = 0$ until the peak (30 s) the flame is propagating within the solid fuel bed as new particles of fuel start to burn. At the peak, there are more fuel particles that have burnt out than new fuel particles burning, and a decay in the mass loss rate is observed, until total burn-out at $t = 55$ s. As seen in Fig. 8, there is no 'stationary moment' in the process.

4.5. Change in the temperature within the flame along the x axis

In Figs. 9–12 we give the change in temperature according to time for various heights x. The numerical results found by the two models of combustion are compared with the experimental results.

The energy released by the combustion of the products of pyrolysis causes a considerable heating of the gas mixture in the fire. These gases thus expand and their density becomes much lower than the density of the ambient air, so they move because of buoyancy forces. These hot gases have an upswing and create a depression (air drainage). This induces an aspiration of fresh air in the horizontal plane, which leads to progressive cooling of hot gases as they rise. This phenomenon makes it possible to bring oxygen to the medium, which is essential to combustion. Moreover, the hot gases are produced "below" the fresh ambient air, which creates instabilities in the flow of air and gases (the fresh gases go down while the hot gases go up). These flows become turbulent at a certain height from the top of the basket. What is usually called the flame is in fact the visible part of these hot gases.

The general shape of all the curves is roughly the same. Thus, one sees first an increasing phase corresponding to the approach of the flame of the thermocouple. In the second zone, the temperature fluctuates around an average value that corresponds to the immersion of the thermocouple in the flame. In the third part, the temperature slowly decreases to reach the ambient temperature.

The comparison between the numerical profiles and the experimental results shows a good agreement at the beginning of

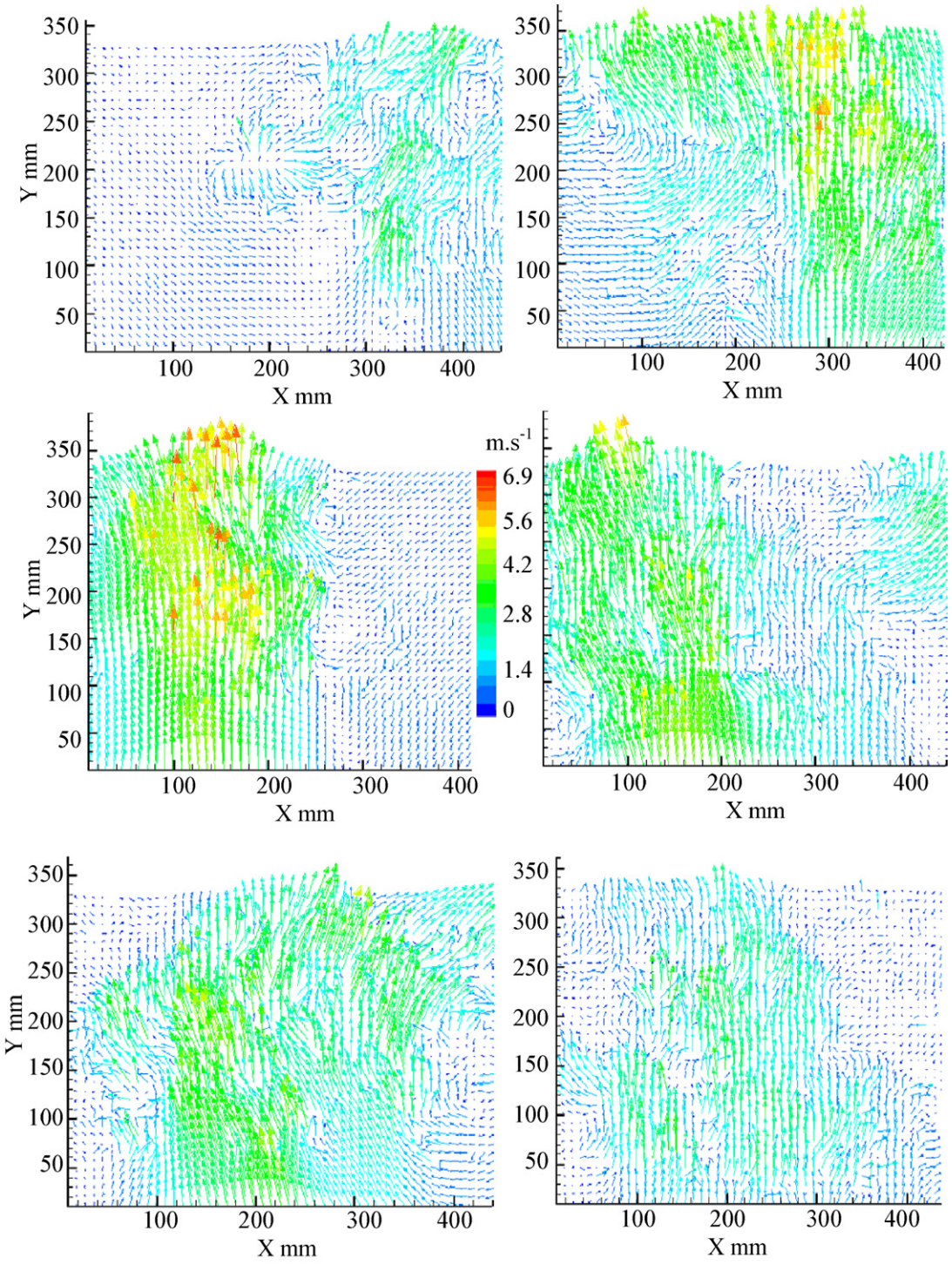

Fig. 6. Unsteady stages of flame propagation.

the combustion and during the time of regeneration. In addition, the results obtained by the β-PDF model are closer to those found in the experiments, while the EDC model overestimates the temperature in these zones.

In Fig. 13 we present the change of temperature on the x axis according to the height of the flame for different time t. We notice that the maximal temperature is located at $x = 20$ cm height, which proves that the temperature within the flame is not homogeneous. The temperature thus increases with height until the maximum is reached, and then decreases rather quickly towards the top of the flame.

4.6. Change of temperature according to the thickness of the flame

The following discussion is devoted to the study of the temperature of the flame according to its thickness. Figs. 14 and 15 reveal the change of the temperature according to time, in hori-

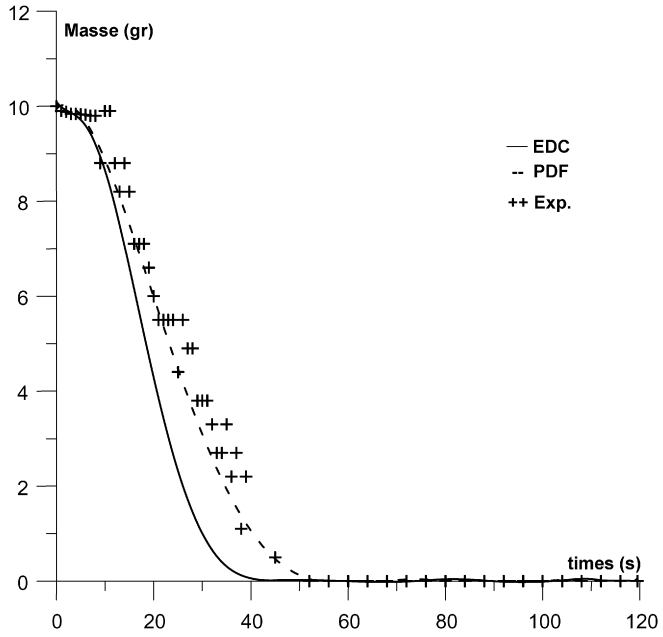

Fig. 7. Profiles of mass loss.

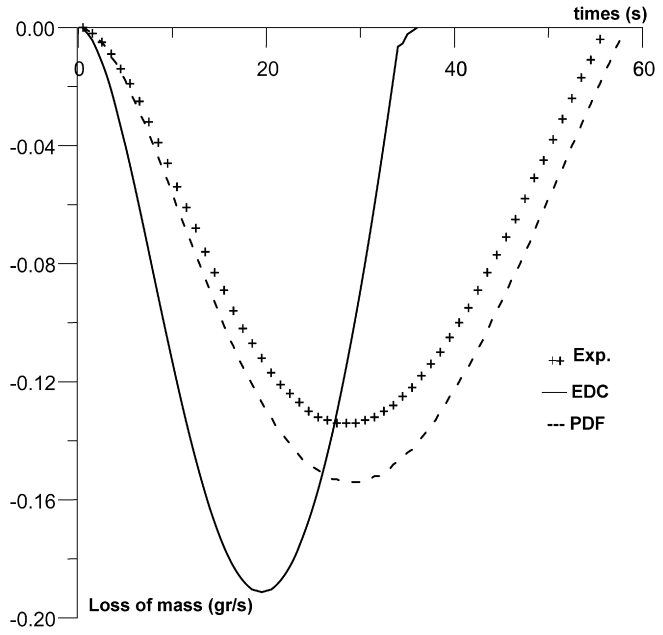

Fig. 8. Profiles of rate of mass loss.

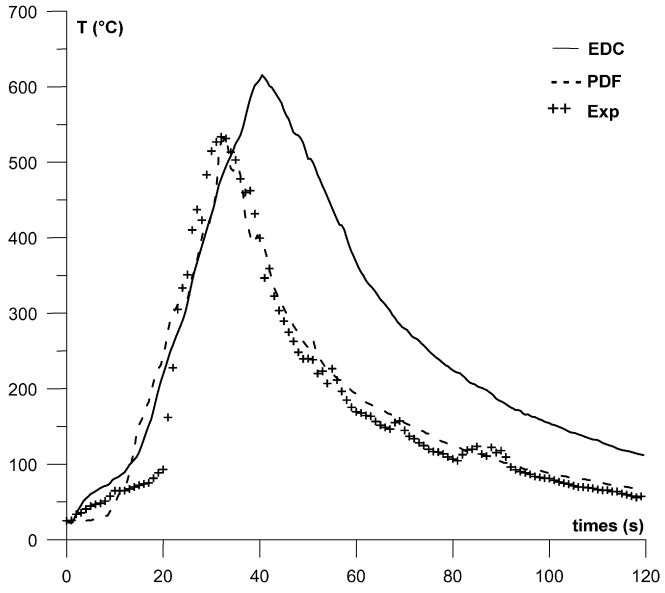

Fig. 9. Temperature at a 5 cm height above the basket top.

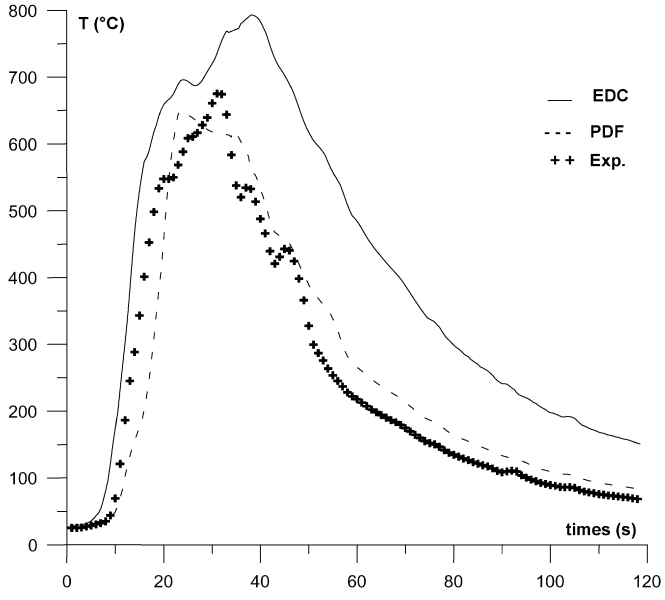

Fig. 10. Temperature at a 15 cm height above the basket top.

zontal planes located at 15 and 20 cm from the top of the basket. The temperatures are measured at 0, 1, 3 and 4 cm from the axis of the basket. The numerical results presented are obtained by the β-PDF model which, based on previous discussion, seems to be a more suitable model. (Solving for the transport equation of the probability density function (PDF) [28,29] represents an attractive approach, because it contains the full statistical information.)

Fig. 16 shows the change of temperature in a horizontal plane located at 20 cm from the top of the basket, according to the radial distance from the basket y, for various times. The general behaviour for different times is roughly the same. We see that the more we move away from the centre of the flame, the more the temperature decreases. Thus, the maxima of temperature are reached in the centre of the fire, which appears logical because it is inside the flame where the physicochemical reactions are formed.

4.7. Distribution of the heat flux received by the vertical planes

Fig. 17 presents the distribution of the heat flux received by vertical planes (xz planes) located at distances respectively equal to $y = 0.5$ m, $y = 1$ m, $y = 2$ m and $y = 4$ m starting from the centre of the basket. Without the presence of wind, this power is of the radiative type. It decreases when the distance between the basket and the plane increases. The maximum heat

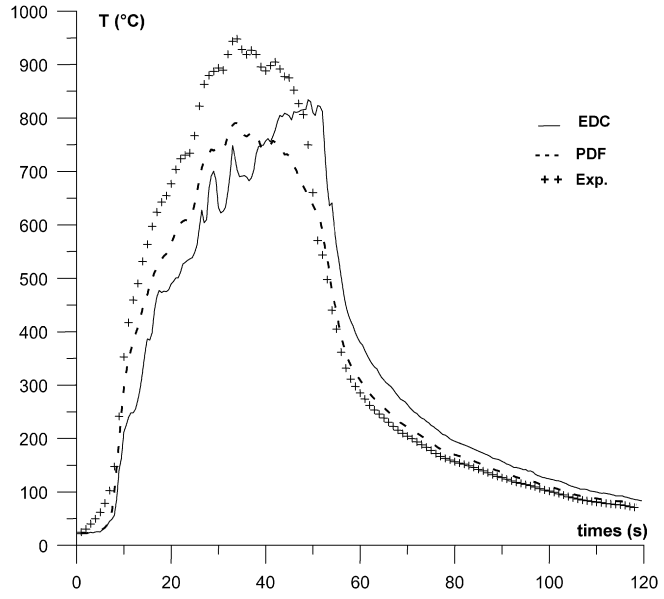

Fig. 11. Temperature at a 20 cm height above the basket top.

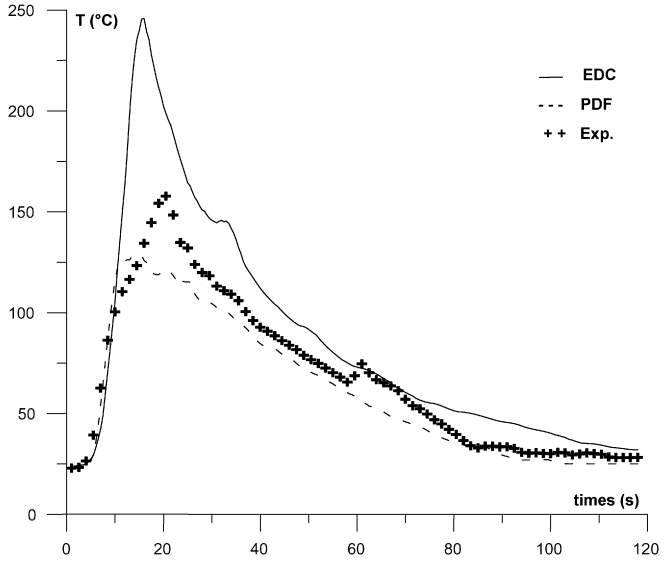

Fig. 12. Temperature at a 60 cm height above the basket top.

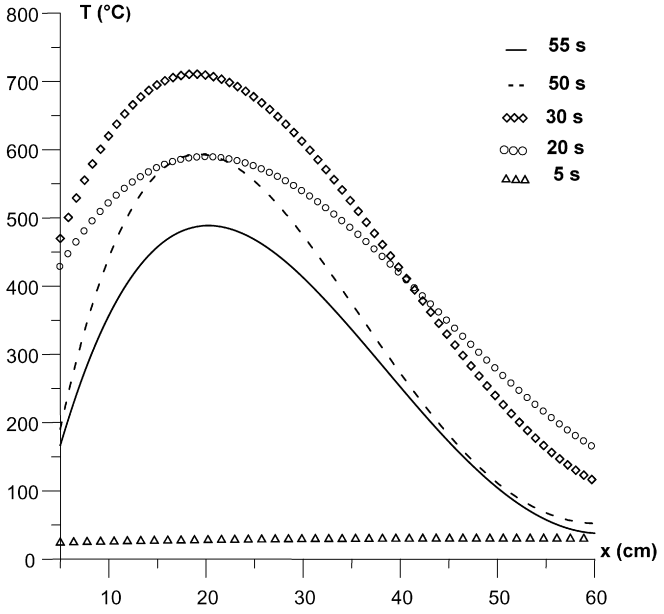

Fig. 13. Temperature profiles of the flame on the basket axis.

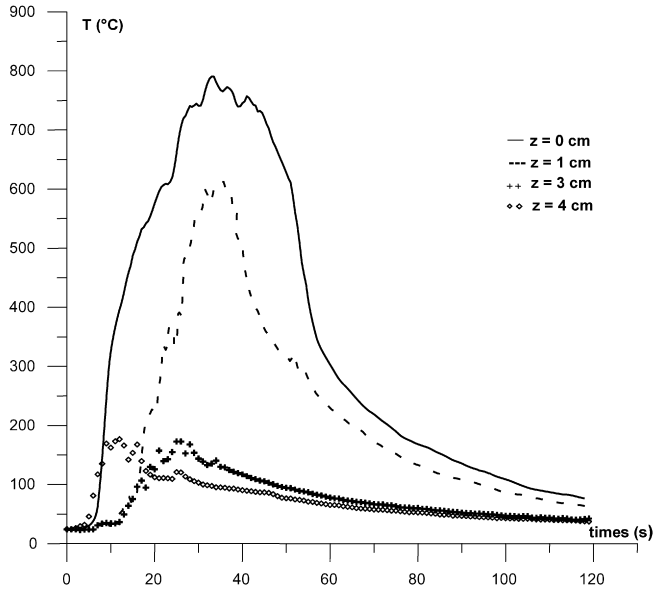

Fig. 14. Temperature profiles in a horizontal plane located 15 cm above the basket top.

flux received by the planes is recorded after approximately 20 s of the release of the flame. It is also noted that the received power is almost nil at a distance of 4 m from the axis. The fluxes received for all the planes cancel at about 50 s, a time which corresponds to the extinction of the flame.

Fig. 18 shows the time-dependent temperature in a horizontal plane, at $x = 20$ cm, for five tests, the second being carried ten minutes after the first. It is noted that the maximum temperature is not the same for all five tests. It is also noted that the stationary phase of test 5 is much longer (50 s) than test 2 (30 s). The experiments were carried out in the same conditions from a climatic point of view (temperature and moisture inside the room did not change during the ten minutes) and also we used the same mass of pine needles. This thus enables us to conclude, after several tests, that the phenomenon of combustion is not reproducible. That is why the results presented in previous figures are the averages of five tests.

5. Conclusion

This work enabled us to study the behaviour of a flame resulting from the combustion of pine needles using experiments as well as numerical models. This behaviour shows three significant phases: the first phase corresponds to the ignition and it is followed by a stationary phase during which the flame keeps practically the same height. The third phase is a phase of degeneration of the flame and its extinction. The maxima of temperature within the flame are reached on the axis for a height $x = 20$ cm. We found that the temperature is a function

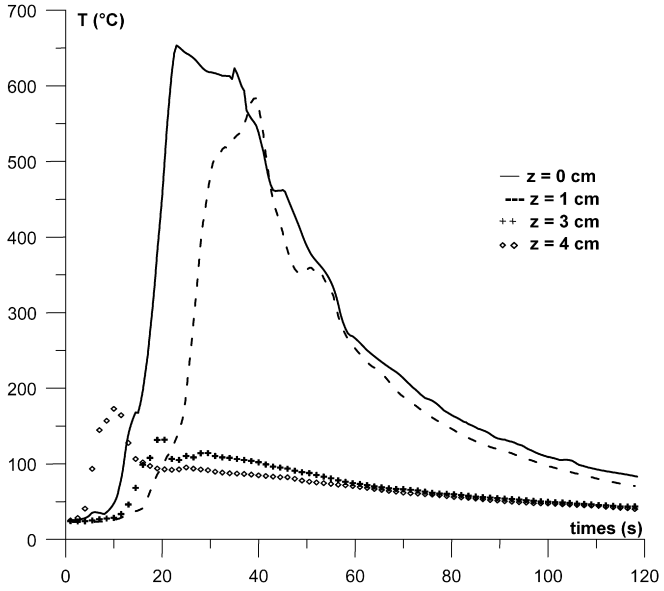

Fig. 15. Temperature profiles in a horizontal plane located 20 cm above the basket top.

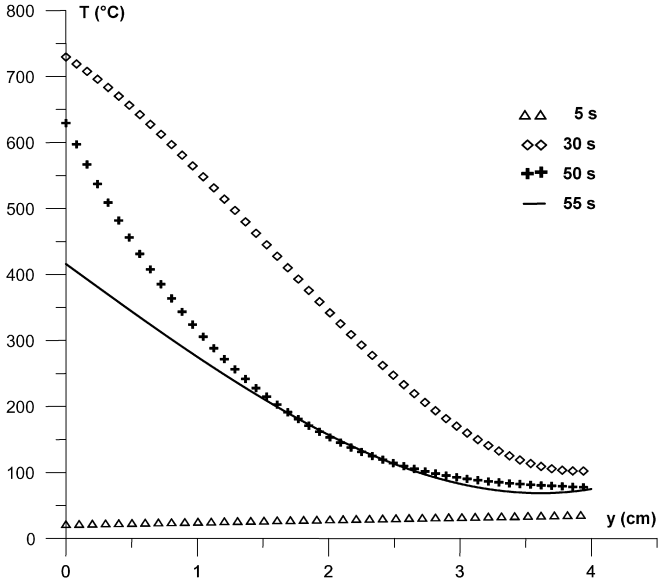

Fig. 16. Temperature profiles in a horizontal plane located 20 cm from the basket top.

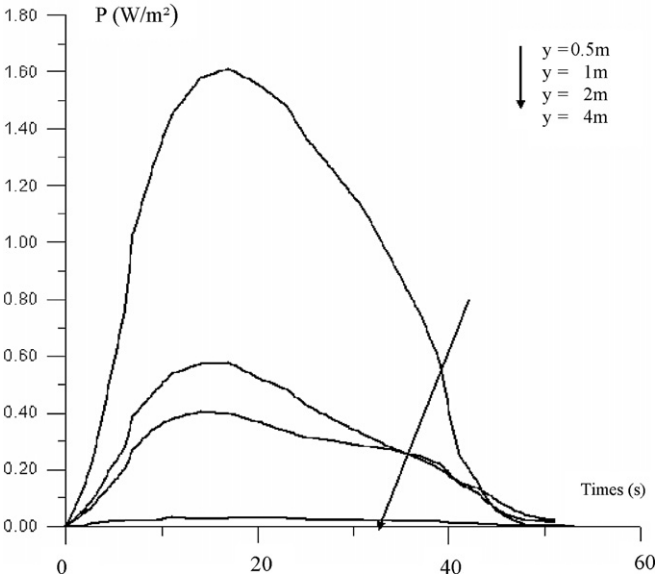

Fig. 17. Distribution of the received flux.

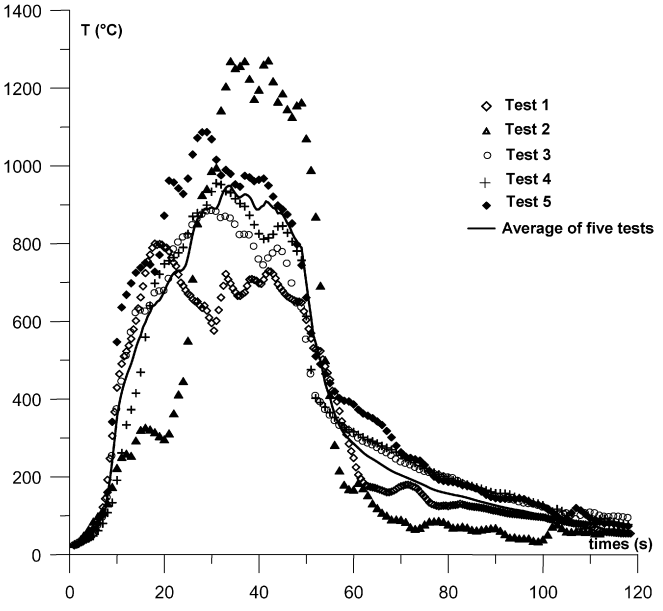

Fig. 18. Comparison of tests in a horizontal plane at 20 cm height.

of the increasing height of the flame until this maximum, and then decreases rather quickly towards the top of the flame. The measured temperatures on horizontal planes show that the maxima are recorded in the axis of the cylindrical basket, which proves that the temperature within the flame is not homogeneous. We noted that, without wind, the power received by planes parallel to the flame cancels itself at approximately 4 m from the axis of the basket. This work also allowed us to analyse the validity of two models of combustion (EDC and β-PDF models) which were developed in order to describe the thermal quantities of the flow. The comparison with experimental results clearly shows that the β-PDF model seems more suitable.

References

[1] L. Naville, Etude expérimentale et modélisation de la propagation d'une flamme sur un combustible poreux : Application aux feux de végétation, Thèse de l'université Aix-Marseille II, 1997.

[2] J. Margerit, Modélisation et simulations numériques de la propagation de feux de forêts, Thèse de l'Institut National Polytechnique de Lorraine, 1998.

[3] R.C. Rothermel, A mathematical model for predicting fire spread in wildland fuels, USDA Forest Service Research paper INT-115, Ogden, UT, 1972, p. 40.

[4] R.O. Weber, Modelling fire spread through fuel beds, Prog. Energy Combust. Sci. 17 (1991) 67.

[5] E.A. Catchpole, N.J. De Mestre, Physical models for a spreading line fire, Aust. Forestry 49 (1986) 102.

[6] P.H. Thomas, Some aspects of the growth and spread of fire in the open, Forestry 40 (1967) 139–164.

[7] R.O. Weber, Analytical models for fire spread due to radiation, Combust. Flame 78 (1989) 398–408.
[8] F.A. Albini, A model for fire spread in wildland fuels by radiation, Combust. Sci. Technol. 42 (1985) 229–258.
[9] A.M. Grishin, in: F. Albini (Ed.), Mathematical Modeling of Forest Fires and New Methods of Fighting Them, Tomsk University, Tomsk, 1997.
[10] M. Larini, F. Giroud, B. Porterie, J.C. Loraud, A multiphase formulation for fire propagation in heterogeneous combustible media, Int. J. Heat Mass Transfer 41 (1998) 881.
[11] R.R. Linn, F.H. Harlow, Use of transport models for wildfire behavior simulations, in: D.X. Viegas (Ed.), Proceedings of the 3rd International Conference on Forest Fire Research, Luso, Portugal, ADAI, University of Coimbra, Portugal, 1998, pp. 363–372.
[12] D. Morvan, J.L. Dupuy, Modeling of fire spread through a forest fuel bed using a multiphase formulation, Combust. Flame (2001) 1981–1994.
[13] A.M. Grishin, A.N. Golovanov, L.Yu. Kataeva, E.L. Loboda, Combust. Explosion Shock Waves 37 (1) (2001) 57.
[14] E.A. Catchpole, W.R. Catchpole, R.C. Rothermel, Int. J. Wildland Fire 3 (1) (1993) 45.
[15] D. Morvan, J.L. Dupuy, Modeling the propagation of a wildfire through a Mediterranean shrub using a multiphase formulation, Combust. Flame 138 (2004) 199–210.
[16] B.F. Magnussen, H. Hjertager, On mathematical modelling of turbulent combustion with special emphasis on soot formation and combustion, in: Proceedings 16th Symposium (International) on Combustion Institute, 1976, pp. 719–729.
[17] B.F. Magnussen, On the structure of turbulence and a generalized eddy dissipation concept for chemical reaction in turbulent flow, in: Nineteenth AIAA Meeting, St. Louis, 1981.
[18] C. Dopazo, Fundamentals of PDF approach for turbulent combustion, part I—basic concepts, part II—an application to diffusion flames, Von Karman Institute for Fluid Dynamics, lecture series, Combustion and two phase flows, February 1996.
[19] R. Borghi, M. Destriau, La combustion et les flammes, Techni 1995, p. 373.
[20] G. Cox, R. Chitty, Combust. Flame 60 (1985) 219.
[21] J.L. Dupuy, Int. J. Wildland Fire 5 (3) (1995) 153–164.
[22] C. Moro, Détermination des caractéristiques physiques de particules de quelques espèces forestières mediterraneennes, Institut National de la Recherche Agronomique, Equipe de Prévention des Incendies de Forêt, Document PIF2006-06.
[23] G. Cox, Combustion Fundamentals of Fires, Academic Press, San Diego, CA, 1996.
[24] R. Borghi, M. Champion, Modélisation et théorie des flammes, Editions Technip, 2000.
[25] N. Mahjoub Said, H. Mhiri, S. El Golli, G. Le Palec, Ph. Bournot, Three-dimensional numerical calculations of a jet in an external cross flow: application of dispersion of pollutants, J. Heat Transfer Trans. ASME 125 (April 2003) 1–13.
[26] B. Porterie, D. Morvan, J.C. Loraud, M. Larini, Firespread through fuel beds: modeling of wind-aided fires and induced hydrodynamics, Phys. Fluids 12 (2000).
[27] S.V. Patankar, Numerical Heat Transfer and Fluid Flow, McGraw-Hill, New York, 1980.
[28] T. Hulek, R.P. Lindstedt, Computations of steady-state and transient premixed turbulent flames using pdf methods, Combust. Flame 104 (1996) 481–504.
[29] S.B. Pope, A. Monte, Carlo method for the pdf equations of turbulent reactive flow, Combust. Sci. Technol. 25 (1981) 159–174.